Available online at www.sciencedirect.com
SCIENCE DIRECT®
Physica D 186 (2003) 20–26
PHYSICA D
www.elsevier.com/locate/physd

Breathers in one-dimensional nonlinear thermalized lattice with an energy gap

M. Eleftheriou [a,*], S. Flach [b], G.P. Tsironis [a]

[a] *Department of Physics, University of Crete and Foundation for Research and Technology-Hellas, P.O. Box 2208, 71003 Heraklion, Crete, Greece*
[b] *Max Planck Institute for the Physics of Complex Systems, Nothnitzer Str. 38, D-01187 Dresden, Germany*

Received 8 February 2003; received in revised form 4 July 2003; accepted 6 July 2003
Communicated by I. Gabitov

Abstract

We study a model of a nonlinear lattice with an on-site potential that induces a breather gap, i.e. a frequency interval where breathers are unstable. The gap is determined numerically and after thermalization of the system we compute power spectra of local displacements. We find that the gap is clearly manifested at small couplings through a large spectral contribution in the linearized phonon region that is not shifted strongly with temperature.

PACS: 63.20.Pw

Keywords: Breathers; Spectral gap

1. Introduction

Discrete breathers (DBs) exist in several nonlinear models with or without on-site potentials. One important condition for the existence of DBs in lattices with nonlinear on-site potentials is that their frequency and all its harmonics lies outside the phonon spectrum [1–3]. Nevertheless it is known that for some families of DBs a gap may occur in their energy as a function of amplitude or frequency [4]. For example, in three-dimensional lattices there is a spectral gap, and as a result in order to excite breathers it is necessary to overcome the energy threshold. This aspect can be useful in a real experiment for the detection of breathers. In this study we attempt to find observable signatures of breathers in a Hamiltonian thermalized lattice that is a nontrivial task [5,6], especially due to the fact that breathers are not easily distinguished from other anharmonic modes. In other studies [7a,7b,8], where a nonlinear thermalized lattice is connected to a zero-temperature heat bath through damping in the boundaries, specific indications of breather modes where found.

In the present work, we search for the conditions that must be fulfilled in an experiment in order to be able to detect breathers. We use a one-dimensional chain with on-site potentials that may induce a spectral gap, in the sense that lower frequency breathers may not be stable while at higher frequencies (or corresponding amplitudes), breathers become stable. In

* Corresponding author. Tel.: +30-810394163; fax: +30-810394101.
E-mail address: marel@physics.uoc.gr (M. Eleftheriou).

0167-2789/$ – see front matter © 2003 Elsevier B.V. All rights reserved.
doi:10.1016/S0167-2789(03)00243-4

Section 2 we analyze the presence of the spectral gap, in Section 3 we thermalize the lattice and obtain numerically the spectra, in Section 4 we study the lattice energy correlations while in Section 5 we conclude.

2. Gap determination

We consider a one-dimensional periodic chain of coupled nonlinear oscillators with the following Hamiltonian:

$$H = \sum_{i=1}^{N} \left[\frac{p_i^2}{2} + V(x_i) + \frac{k}{2}(x_i - x_{i+1})^2 \right], \qquad (1)$$

where x_i and p_i are the displacement and the momentum of the ith site from the equilibrium position, respectively, and the on-site potential is a nonlinear ϕ^8 hard potential, i.e. $V(x) = x^2/2 + x^8/8$. The parameter k determines the strength of the nearest-neighbor interaction. For the hard ϕ^8 on-site potential and for coupling $k = 0.1$, we construct breathers using the anticontinuous limit method [1,2]. For our choice of parameters the phonon band lies in the range $[\omega_0, \omega_\pi] = [1, 1.18]$ where $\omega_0 \equiv \omega(q = 0) = 1$, $\omega_\pi \equiv \omega(q = \pi) = 1.18$ where q is the dimensionless wavenumber. We look for breathers with frequency $\omega_b > \omega_\pi$ and we find two types of them: those with frequencies in the interval $(\omega_\pi, \omega_b^{\min}) = (1.18, 1.243)$ are not stable, while breathers that have frequencies $\omega_b > \omega_b^{\min}$ are found to be stable. The stability was checked through time evolutions and as well as the analysis of the DB Floquet spectrum. Specifically for breathers that have frequencies belonging to the gap $(\omega_\pi, \omega_b^{\min})$, one pair of Floquet eigenvalues lies outside the unit circle in contrast to those breathers with frequencies $\omega_b > \omega_b^{\min}$ for which all eigenvalues lie on the unit circle; we thus found that the lower limit for a breather to be stable is $\omega_b^{\min}$. Also we performed time evolutions for several breathers constructed using the anticontinuous method. For example, we observe that a breather with frequency $\omega_b = 1.207$ starts to lose its shape in approximately 115 breather periods (T_b) with random

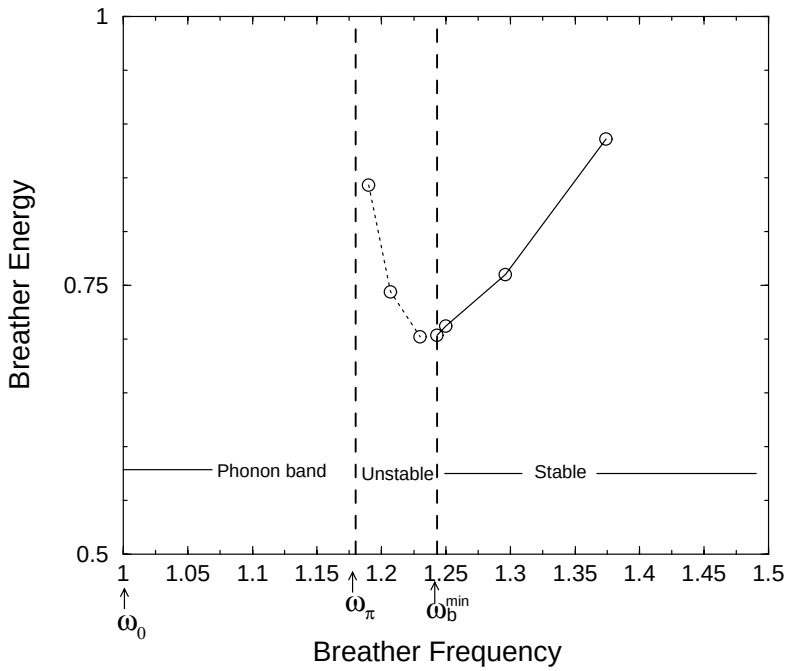

Fig. 1. For coupling $k = 0.1$ we plot the breather energy as a function of its frequency. The phonon band lies in the frequency range $(\omega_0, \omega_\pi) = (1, 1.18)$ while the breather instability gap is in the range $(\omega_\pi, \omega_b^{\min}) = (1.18, 1.243)$. For $\omega > \omega_b^{\min}$ breathers are stable.

Table 1
In the first column is the coupling k, in the second and third are the frequencies of the lower limit (wavenumber $q = 0$) and the upper limit (wavenumber $q = \pi$) of the phonon band, respectively, and in the last two columns we place the frequency ($\omega_b^{\min}$) and the corresponding energy ($E_b^{\min}$) that mark the onset of the breather stability regime[a]

k	ω_0	ω_π	$\omega_b^{\min}$	$E_b^{\min}$
0.1	1	1.18	1.243	0.7036
0.2	1	1.34	1.42	1.147
0.3	1	1.48	1.59	1.6136
0.4	1	1.612	1.754	2.1098
0.5	1	1.732	1.881	2.62
1	1	2.236	2.47	5.55

[a] For each value of the coupling the breather frequency gap is located between ω_π and $\omega_b^{\min}$.

perturbation of the order of 10^{-12}, while a breather with frequency $\omega_b = 1.374$ remains stable at time $t \geq 1093T_b$ with a perturbation of the order of 10^{-3}.

In Fig. 1 two branches appear in the plot of energy as a function of the frequency. In the first branch where the energy decreases with increasing frequency (or amplitude), breathers are unstable. For larger frequencies a second branch of stable breathers appears with energy being an increasing function of frequency. We also note that for a breather with coupling $k = 0.1$ and frequency $\omega_b^{\min} = 1.243$ (that is the upper limit of the gap) its energy is $E_b^{\min} = 0.7036$ the breather is mainly localized on three sites. Thus the minimum stable breather energy per degree of freedom is $E_b^{\min}/3 = 0.234$ in this particular model. Analogous results are found for higher values of coupling such as $k = 0.2$ and further, i.e. breathers are not stable in a specific interval of frequencies while higher frequency breathers are stable; these features are tabulated in Table 1. The gaps have been determined through evaluation of Floquet spectra of the linearized modes around the DBs.

3. Thermalization and Fourier spectra

After having examined the breather regimes in the Hamiltonian case we now bring the system in contact with a bath of temperature T. This is done by introducing stochastic forces and damping in each oscillator and following the time evolution of the resulting coupled Langevin equations. The dissipation value we use is $\gamma = 0.01$ and this value controls the time scale for relaxation. When the system reaches equilibrium defined through equipartition and obtained when the kinetic energy per particle is approximately equal to $k_B T/2$, we remove completely the heat bath and study the evolving initially thermalized Hamiltonian system. We compute the time correlation of the local displacements as well as their Fourier transforms. We treat a lattice of $N = 100$ sites and present our results for different couplings in Fig. 2 ($k = 0.1$) and in Fig. 3 ($k = 0.5, 1$); as we will see below the coupling plays a crucial role. For each temperature we run n different realizations (typically $n = 50$) and compute the average in the correlation of displacements that are taken after a long transient of time to ensure thermal equilibrium. The quantity we evaluate is

$$S(t) = \frac{1}{N}\left[\frac{1}{t_{\rm fin} - t_{\rm in}} \sum_{i=1}^{N} \int_{t_{\rm in}}^{t_{\rm fin}} \langle x_i(t+t')x_i(t')\rangle \, {\rm d}t'\right], \tag{2}$$

where $t_{\rm in} = 2000$ and $t_{\rm fin} = 2500$ while the integral in Eq. (2) is actually a sum with ${\rm d}t' = 0.1$. The Fourier transform of $S(t)$ is

$$S(\omega_m) = \Delta t \sum_{j=0}^{(t_{\rm fin}/\Delta t)-1} {\rm e}^{-(2\pi {\rm i}/t_{\rm fin})m\Delta t j} \, S(\Delta t j), \tag{3}$$

where $\omega_m = 2\pi m/t_{\rm fin}, m = 0, 1, \ldots, (1/2)(t_{\rm fin}/\Delta t) - 1$. Finally the power spectrum of the correlation $S(t)$ is given by

$$P(\omega) = ({\rm Re}(S(\omega)))^2 + ({\rm Im}(S(\omega)))^2, \tag{4}$$

where ${\rm Re}(S(\omega))$ and ${\rm Im}(S(\omega))$ denote the real and imaginary part, respectively.

In Fig. 2 we plot the power spectra for the hard ϕ^8 potential and compare them to the hard ϕ^4 on-site potential $V(x) = x^2/2 + x^4/4$ using the same coupling $k = 0.1$. At low temperatures, in both cases, only phonons are excited since essentially all modes excited in this temperature regime are linear phonon modes inside the phonon band (Fig. 2(a)). On the other hand when the temperature is increased, in addition to phonons nonlinear modes are also excited, and

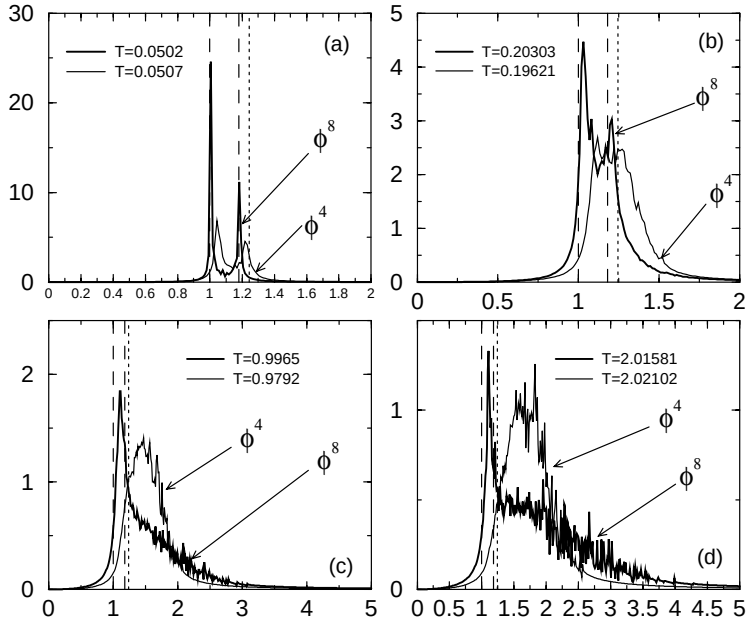

Fig. 2. Power spectra as a function of frequency for $k = 0.1$ and different temperatures. The range between the two dashed lines denotes the phonon band while the breather gap is located between the upper dashed line and the dotted line. Dark intense lines correspond to the hard ϕ^8 and lighter lines to the hard ϕ^4 cases. In subgraphs (a)–(d) temperatures for hard ϕ^8 and hard ϕ^4 cases are not exactly equal due to the fact that temperature is calculated for each run from the equipartition theorem. Position–position correlations $S(t)$'s are normalized to unity in all the cases and also the integral below the curve of $P(\omega)$ is normalized in such a way that is a unity in all the cases as well.

as a result the Fourier spectra become broader (Fig. 2 (b)–(d)). Analysis of the spectra changes as a function of temperature shows a clear deviation in the behavior of the two systems in the spectral region where the ϕ^8 breather gap is located. Specifically, as the temperature grows ($T \geq 1$) we observe that in the region of the breather gap the spectral intensity of the ϕ^8 potential drops while the intensity in the linear region increases.

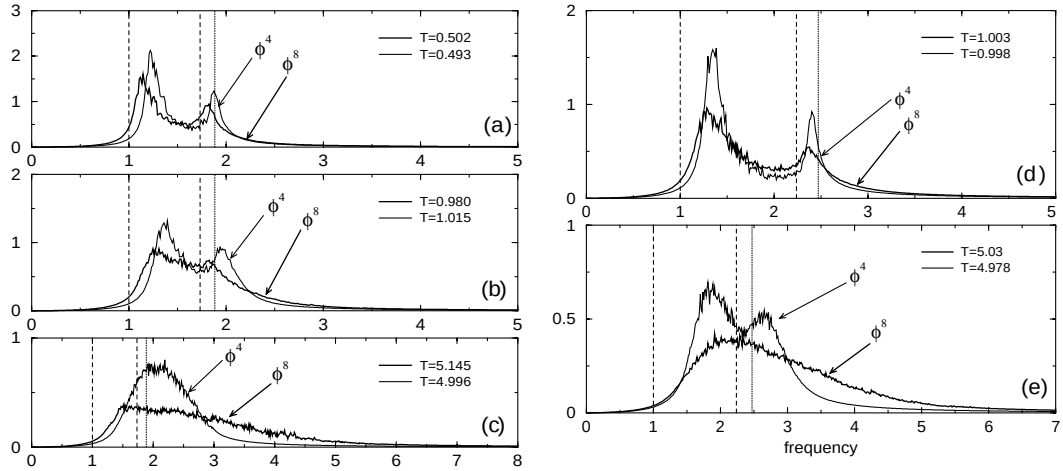

Fig. 3. Power spectrum $P(\omega)$ as a function of frequency. Left panel: $k = 0.5$ for different temperatures in (a)–(c); right panel: $k = 1$ in (d) and (e). Other notations are as in Fig. 2.

This is marked contrast to the ϕ^4 system where we observe a continuous depletion of the linearized vibrational region accompanied by a global shift to higher frequencies. For instance, we observe in Fig. 2(b) that for energy $k_B T = 0.2027$ ($k_B = 1$) that is near the critical value E_b^{min} $(k = 0.1)/3 = 0.234$ the two spectra already exhibit the different trend. We thus observe that the hard ϕ^4 on-site potential exhibits a continuous spectral displacement to larger frequencies induced by the increased presence of breather modes in the lattice while in the hard ϕ^8 case the breather gap acts as a spectral barrier, a feature that is understood as follows: as temperature increases there is increased tendency for breather formation. However, since breathers in the gap region are unstable, they quickly break up after formation and most of them become phonons. As a result, there is a decrease in the intensity in the breather gap region that is moved partially in the phonon range. This feature is clearly manifested in Fig. 2(c) and (d) where the excess intensity in the phonon region is accompanied by a drastic drop in the breather gap region. We attribute this asymmetry precisely to the transfer of spectral intensity from the breather gap region to smaller frequencies.

For larger values of coupling, i.e. $k = 0.5$ and 1, respectively, the phenomenon of intensity increase in the phonon region is not observed. For instance, for $k = 0.5$ (Fig. 3) and using Table 1 we expect the gap to be located in the range $\omega_\pi = 1.732$ to $\omega_b^{min} = 1.881$. As can be readily seen in Fig. 3 where this range is delimited by a dashed (upper) and dotted lines no substantial reduction of intensity is observed in this range with a simultaneous increase of the intensity in the phonon range. A similar behavior is seen also at the even larger coupling $k = 1$. As a result, the spectral analysis that preceded marks two different tendencies. While the system is close to the anticontinuous limit (small coupling) breathers are indeed generated in both ϕ^4 and ϕ^8 models. In the latter case however breathers are unstable in the gap region and as a result there is a depletion of intensity in this region making the gap discernible in contrast to the gapless ϕ^4

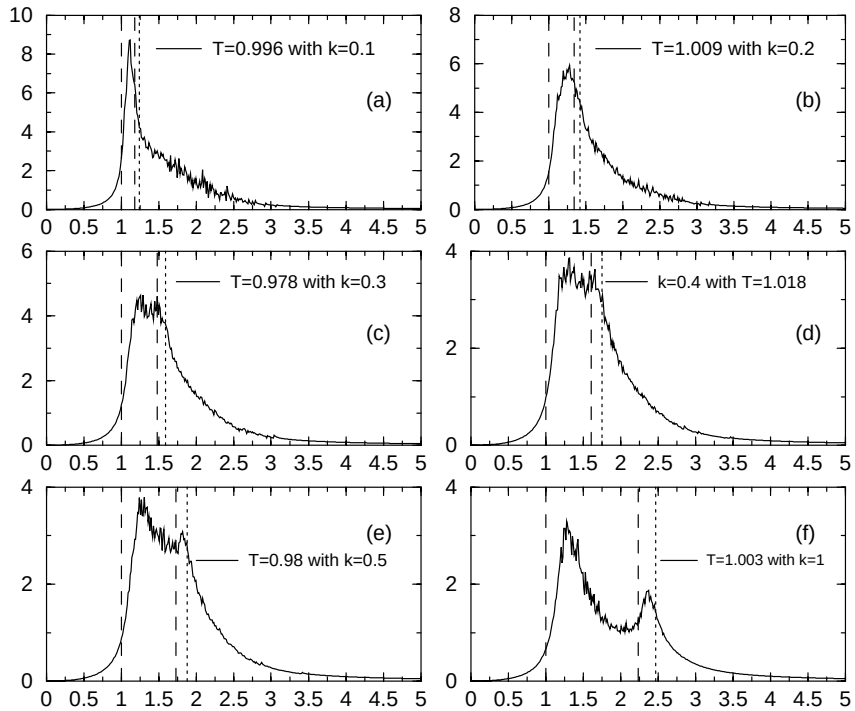

Fig. 4. Power spectra as a function of frequency for various couplings and the hard ϕ^8 on-site potential. The temperature is $T \approx 1$, and the coupling is indicated in each subgraph.

case. As the coupling increases however the nonlinear modes generated become broad and as a result the existence of a breather gap in the ϕ^8 model becomes moat. Both models have compatible behavior. We thus conclude that the distinct spectral signature of the breather gap of intensity accumulation in the phonon range is only observable at small couplings close to the anticontinuous limit. This aspect is further exemplified in Fig. 4, where power spectra for different values of coupling are presented and show a different change as coupling increases. For $k = 0.4$ and larger coupling values the gap is not visible anymore.

4. Energy correlations

In order to substantiate the regimes where breathers are important in the previous observations we perform a series of numerical experiments in the time domain. Specifically we compute time dependent local energy correlation functions for both ϕ^4 and ϕ^8 models using various coupling values. In particular we evaluate time dependent local energy correlation functions for the linear ϕ^2 model, viz., $V(x) = x^2/2$, hard ϕ^4 and hard ϕ^8 on-site potentials. We use a lattice with $N = 100$ sites and perform $n = 100$ realizations for each temperature (the dissipation for the thermalization was set again $\gamma = 0.01$). We introduce the local energy at each site as

$$E_i = \tfrac{1}{2}p_i^2 + V(x_i) + \tfrac{1}{4}k(x_i - x_{i+1})^2 + \tfrac{1}{4}k(x_{i-1} - x_i)^2. \quad (5)$$

In Fig. 5 we plot the time correlation function:

$$C(t,0) = \frac{1}{N}\left\langle \sum_{i=1}^{N} E_i(t)E_i(0)\right\rangle - \left\langle \frac{1}{N}\sum_{i=1}^{N} E_i\right\rangle^2 \quad (6)$$

that is normalized to unity.

The time dependent energy correlation function contains the information of how the energy is transferred between the sites. As we can see from Fig. 5 in the case of a purely linear on-site potential it approaches zero while the two nonlinear hard on-site potentials give a slower decay [7a,7b]. In nonlinear lattices, energy spreads out on a slower time scale as compared to the corresponding linear one because of the formation of localized structures, at least in the case of small couplings as in Fig. 5(a) and (b) that contribute to the energy trapping.

From the numerical determination of the correlation function in Fig. 5 we note that as the nonlinearity in the potential grows the decay features change in the small coupling ($k = 0.1$) case (Fig. 5(a) and (b)). Indeed temperature fluctuations induce breather modes that

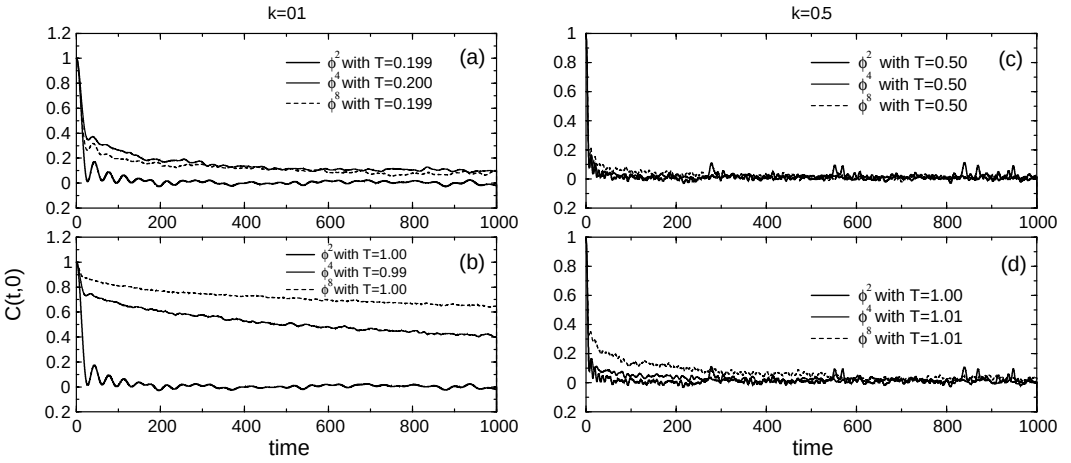

Fig. 5. The energy correlation function $C(t, 0)$ (normalized to unity) as a function of time for the three different on-site potentials. V_1 is the linear, V_2 the hard ϕ^4 and V_3 the hard ϕ^8 potentials as indicated in the labels. For (a) and (b) the coupling is $k = 0.1$ and for (c) and (d) $k = 0.5$.

are clearly more persistent in the ϕ^8 case compared to the ϕ^4 model (Fig. 5(b)). In these time resolved simulations the presence or absence of the breather gap does not play an important role. The slow decay of the correlation function however demonstrates that breathers are indeed present in the corresponding regime, and, as a result, the spectral phenomena explained in the previous section are directly attributed to them. In the high coupling case on the other hand, no correlations persist and as a result breather modes are statistically absent in both low and higher temperature regimes (Fig. 5(c) and (d)). The evaluation thus of the correlation function augments the analysis of the previous section showing that only at small couplings the peculiar spectral behavior of the ϕ^8 model can be attributed to breathers.

5. Conclusions

In the present work we performed numerically a spectral analysis of a nonlinear thermalized lattice constituted of a one-dimensional chain of coupled nonlinear oscillators. We used for each oscillator an on-site potential that depends on the eighth power of the oscillator displacement, i.e. a hard ϕ^8 potential and compared our results with the standard hard ϕ^4 potential. The specific choice of the ϕ^8 potential was dictated by the fact that in this case a breather spectral gap appears just above the phonon band where breather modes are unstable. In this work we focused on the possible manifestation of this frequency gap at finite temperatures. Our analysis demonstrates that there are two regimes depending on the value of the nearest-neighboring coupling k. For small k-values close to the anticontinuous limit we observe from the displacement correlation function a reduced spectral weight in the breather gap region accompanied by a drastic increase of the spectral contribution from the phonon region. This effect that persists to high temperatures is attributed to the decay of DBs of the gap region into phonon modes. This feature is clearly absent in the gapless ϕ^4 on-site potential. The second regime is that of large k-values where the system is far from the anticontinuous limit and resulting nonlinear modes are not DBs. In this last case and in the high temperature regime the correlation spectrum becomes less structured and the breather gap is not manifested. Energy correlation results corroborate the existence of these two distinct regimes at finite temperatures. The fact that increased nonlinearity in the on-site potential leaves a clear signature in the position–position correlation spectrum at weak couplings is attributed directly to breather modes and their properties. As a result this aspect may be manifested also in more complex, real materials that necessarily contain potentials with high nonlinearities.

Acknowledgements

This work was partially supported by the European Union under HPRN-CT-1999-00163.

References

[1] R.S. MacKay, S. Aubry, Nonlinearity 7 (1994) 1623.
[2] S. Aubry, Physica D 71 (1994) 196.
[3] S. Flach, Phys. Rev. E 50 (1994) 3134.
[4] S. Flach, K. Kladko, R.S. MacKay, Phys. Rev. Lett. 78 (1997) 1207.
[5] M. Peyrard, Physica D 119 (1998) 184.
[6] S. Flach, G. Mutschke, Phys. Rev. E 49 (1994) 5018.
[7] (a) G.P. Tsironis, S. Aubry, Phys. Rev. Lett. 77 (1996) 5225; (b) A. Bikaki, N.K. Voulgarakis, S. Aubry, G.P. Tsironis, Phys. Rev. E 59 (1999) 1234.
[8] R. Reigada, A. Sarmiento, K. Lindenberg, Phys. Rev. E 64 (2001) 066608.